Interplay of Correlations and Kohn Anomalies in Three Dimensions: Quantum Criticality with a Twist

T. Schäfer,[1] A. A. Katanin,[2] K. Held,[1] and A. Toschi[1]
[1]Institute of Solid State Physics, Technische Universität Wien, 1040 Vienna, Austria
[2]Institute of Metal Physics, 620990, Kovalevskaya str. 18, Ekaterinburg, Russia
and Ural Federal University, Mira str. 19, 620002 Ekaterinburg, Russia
(Received 25 May 2016; revised manuscript received 28 April 2017; published 26 July 2017)

A general understanding of quantum phase transitions in strongly correlated materials is still lacking. By exploiting a cutting-edge quantum many-body approach, the dynamical vertex approximation, we make important progress, determining the quantum critical properties of the antiferromagnetic transition in the fundamental model for correlated electrons, the Hubbard model in three dimensions. In particular, we demonstrate that—in contradiction to the conventional Hertz-Millis-Moriya theory—its quantum critical behavior is driven by the Kohn anomalies of the Fermi surface, even when electronic correlations become strong.

DOI: 10.1103/PhysRevLett.119.046402

Introduction.—The underlying quantum mechanical nature of the physical world is often elusive at the macroscopic scale of every-day-life phenomena. In the case of solid state physics, the most striking manifestations of its quantum origin are confined to very low temperatures, where thermal fluctuations are frozen. An important exception is realized where thermodynamic phase transitions (e.g., to a magnetic state) are driven to occur at zero temperature, at a quantum critical point (QCP) [1–4]: The corresponding quantum critical fluctuations become then abruptly visible also at sufficiently high temperatures, representing one of the most exciting subjects in condensed matter physics. While QCPs are actually found experimentally in the phase diagrams of several compounds [1], a general theoretical treatment of their physics is still lacking. Consequently, the analysis of experiments often remains based on a mere fitting of the exponents controlling the critical behavior at the QCPs, preventing a general comprehension of the phenomenon. The major challenge, in this respect, is the competition of several equally important physical mechanisms, because, at the QCP, both long-ranged space and time fluctuations must be treated on an equal footing. In fact, this is only possible in limiting cases, such as in the perturbative regime, by means of the Moriya [5]-Dzyaloshinskii-Kondratenko [6] theory and the famous renormalization group (RG) treatment by Hertz [7] and Millis [8]. However, an actual comprehension of the experiments based only on these theories is highly problematic, for two reasons. First of all, most quantum critical materials are strongly correlated. This is certainly the case for the (antiferro)magnetic quantum critical points (QCPs) of transition metals under pressure, such as Cr [9,10] or with doping, $Cr_{1-x}V_x$ [11,12] and heavy fermion compounds under pressure or in a magnetic field, such as in $CeCu_{6-x}Au_x$ [13] and $YbRh_2Si_2$ [14,15]. It has been established that one effect of strong correlations, namely, the breakdown of the "large" Fermi surface containing both conduction and f electrons and the associated local quantum criticality [16,17], may lead to different critical exponents. Nonetheless, we are still far away from identifying the universality classes beyond the conventional Hertz-Millis-Moriya (HMM) theory.

Besides electronic correlations, the physics of QCPs can also be affected by specific properties of their Fermi surfaces (FS), such as van Hove singularities, nesting, or Kohn points. The effects thereof are often of minor importance at high-T, but can be amplified in the low-T regime. While van Hove singularities and nesting require special forms of the electronic spectrum, Kohn points are more generic and easily occur in three-dimensional (3D) [18–20] and two-dimensional (2D) systems [21–23]. Kohn points are defined as the points of the FS that (i) are connected by the spin-density wave (SDW) vector $\mathbf{Q}$ and (ii) beyond that have opposite Fermi velocities. These points are associated with the textbook "Kohn anomalies" of the susceptibilities [18,24], also called $Q = 2k_F$ anomalies, which is the momentum where they occur for an isotropic FS. The effect of Kohn anomalies on the phonon dispersion is well known [18] and the breakdown of standard HMM theory has been conjectured [1,8].

In this Letter we make significant progress towards a better understanding of QCPs. We demonstrate that FS features in three dimensions lead to an unexpected universality class of its magnetic QCP, which also holds in the nonperturbative regime. In principle, the complexity of the competing microscopic mechanisms underlying a quantum phase transition of correlated electrons calls for a quantum many-body technique capable of treating both, extended spatial and temporal fluctuations, beyond the weak-coupling, perturbative regime. The approach we exploit here is the dynamical vertex approximation (DΓA) [25–29],

which is a diagrammatic extension [25,30–39] of dynamical mean field theory (DMFT) [40,41] built on its two-particle vertices [42,43]. It has been already successfully used to study classical, finite temperature criticality of strongly correlated systems in three dimensions [44–46], as well as long-range antiferromagnetic (AFM) fluctuations and their effect on the electronic self-energy in two dimensions [26,47]. In fact, DΓA builds up nonlocal corrections at all length scales on top of DMFT [42], which in turn captures, in a nonperturbative fashion, all purely local temporal correlations [41]. Hence, per construction, the scheme is particularly suited to the study of quantum critical phenomena.

The obtained phase diagram of the 3D Hubbard model as a function of doping displays a progressive suppression of the Néel temperature (T_N), a crossover to an incommensurate SDW order, and eventually the vanishing of the magnetic order at a QCP with ∼20% doping. Upon doping, the critical scaling properties of the second-order magnetic transition change abruptly from the ones expected for the universality class of the 3D Heisenberg model, a "classical" finite-T phase transition, to a quantum critical behavior visible in a relatively broad funnel-shaped temperature region above the QCP. Our results unveil the importance of Kohn anomalies for the scaling properties of the QCP. In particular, the T dependence of the magnetic susceptibility ($\chi_{\mathbf{Q}} \propto T^{-\gamma}$) at the SDW wave vector $\mathbf{Q}$ and of the correlation length ($\xi \propto T^{-\nu}$) largely deviate from the typical behavior expected from the HMM theory for AFM quantum phase transitions in three dimensions.

Phase diagram.—We focus here on the magnetic transitions in the Hubbard model on a simple cubic lattice [48]:

$$H = -t\sum_{\langle ij\rangle\sigma} c^{\dagger}_{i\sigma}c_{j\sigma} + U\sum_{i} n_{i\uparrow}n_{i\downarrow}, \tag{1}$$

where t is the hopping amplitude between nearest neighbors, U the local Coulomb interaction, $c^{\dagger}_{i\sigma}$ ($c_{i\sigma}$) creates (annihilates) an electron with spin $\sigma = \uparrow, \downarrow$ at site i, and $n_{i\sigma} = c^{\dagger}_{i\sigma}c_{i\sigma}$; the average density is $n = \langle n_{i\uparrow}\rangle + \langle n_{i\downarrow}\rangle$. Hereafter, all energies are measured in units of $2\sqrt{6}t$, twice the standard deviation of the noninteracting density of states; we employ $U = 2.0$, for which the highest T_N at half-filling is found in both, DMFT and DΓA [44]. We do not consider phase separation [49], charge ordering [50,51], or disorder-induced effects [52].

To explore the magnetic phase diagram, we employ DMFT with exact diagonalization (ED) as an impurity solver and DΓA in its ladder-approximation version supplemented by Moriyaesque λ-corrections; see Refs. [26,28,53] for the implementation used here as well, see Supplemental Material, Sec. II(ii) for more specific details [54]. This approach includes spin fluctuations and was successfully applied to calculate the critical exponents in three dimensions before [44]. Superconducting fluctuations are treated at the DMFT level (the full parquet DΓA [57,58] which would incorporate these fluctuations is numerically too demanding for the required momentum grids at the QCP).

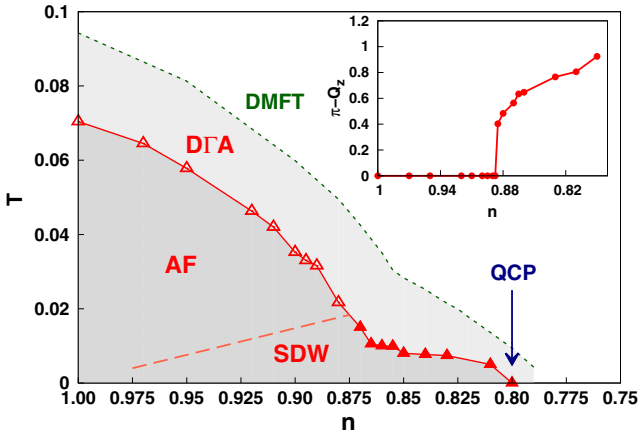

FIG. 1. Phase diagram of the 3D Hubbard model at $U = 2.0$, showing the leading magnetic instability as a function of the density n in both DMFT and DΓA. Inset: Evolution of the magnetic ordering vector along the instability line of DΓA, showing a transition from an commensurate AFM with $Q_z = \pi$ (open triangles in the main panel) to incommensurate SDW with $Q_z < \pi$ (full triangles in the main panel). The dashed red line indicates the presumptive crossover between AFM and SDW.

The primary quantity we calculate is the static, fully momentum-dependent magnetic susceptibility $\chi_{\mathbf{q}} \equiv \chi_{\mathbf{q}}(\omega = 0)$, as a function of temperature T. It has a maximum at a specific (temperature-dependent) wave vector $\mathbf{q} = \mathbf{Q}_T$, and diverges at $T = T_N$, marking the occurrence of a second-order phase transition towards magnetism with ordering vector $\mathbf{Q}_{T_N}$.

Figure 1 shows the corresponding divergence points in the T-n phase-diagram both for DMFT (green) and DΓA (red). By progressively reducing n, T_N decreases and two regions of the magnetic ordering can be distinguished: (i) close to half-filling, we observe an instability at $\mathbf{Q}_{T_N} = (\pi, \pi, \pi)$, i.e., to commensurate AFM (open triangles); (ii) at higher doping ($n \lesssim 0.88$) the ordering vector is shifted to $\mathbf{Q}_{T_N} = (\pi, \pi, Q_z < \pi)$, i.e., an incommensurate SDW (filled triangles). The inset of Fig. 1 quantifies the incommensurability $\pi - Q_z$, i.e., the deviation from a checkerboard AFM order.

Eventually, ordering is suppressed completely as $T_N \to 0$, leading to the emergence of a QCP at $n_c^{\mathrm{D\Gamma A}} \approx 0.805$. We note that the critical filling in DMFT is comparable to that obtained before [59] for a similar interaction strength ($U = 2.04$).

Critical properties.—Let us now turn to the (quantum) critical behavior. We select representative temperature cuts at four different dopings ($n = 1.0/0.87/0.805/0.79$) chosen on both the ordered and the disordered side of the QCP. Along these four paths we compute two fundamental observables, which yield the (quantum) critical exponents γ and ν of the magnetic transition: (i) the spin

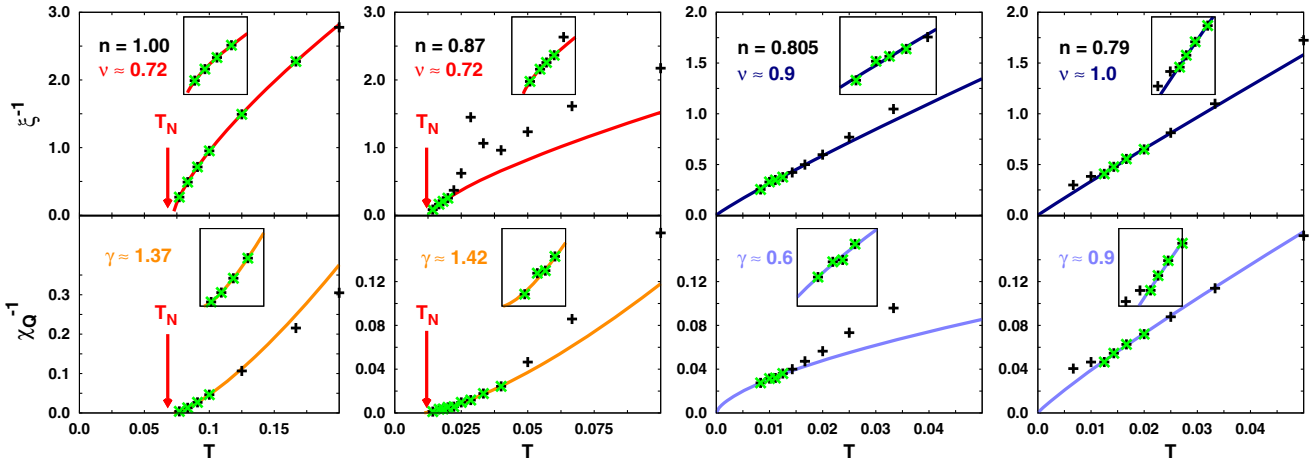

FIG. 2. Inverse correlation length (ξ^{-1}, upper panels) and susceptibility ($\chi_{\mathbf{Q}}^{-1}$, lower panels) computed in DΓA as a function of T for different n. The solid lines show the fits for extracting the critical exponents ν and γ (using the respective green points). The insets show enlargements of the four respective lowest temperature points.

susceptibility $\chi_{\mathbf{Q}_T} \propto (T - T_N)^{-\gamma}$ at its maximum, reached at the T-dependent wave vector $\mathbf{Q}_T$, and (ii) the corresponding correlation length $\xi \propto (T - T_N)^{-\nu}$. The latter is calculated via $\chi_{\mathbf{Q}_T+\mathbf{q}} = A(\mathbf{q}^2 + \xi^{-2})^{-1}$.

Figure 2 shows the T dependence of ξ^{-1} (upper panels) and $\chi_{\mathbf{Q}_T}^{-1}$ (lower panels). Note that, apart from its intrinsic T dependence, the susceptibility is also affected by the T dependence of the wave vector $\mathbf{Q}_T$, with the further complication that the dominating wave vector changes with both n and T.

In the half-filled case (leftmost panels of Fig. 2) both ξ and $\chi_{\mathbf{Q}_T}$ display a critical behavior compatible with the 3D Heisenberg universality class when approaching the classical (finite-T) antiferromagnetic phase transition at $T_N(n = 1) \approx 0.072$. The numerically extracted critical exponents of $\nu \approx 0.72$ and $\gamma \approx 1.37$ are consistent with previous calculations [44,46]; cf. our overview in Fig. 3 below.

Significant changes are observed at a doping, where the SDW order appears ($n \simeq 0.87$, second column of Fig. 2). Here, by inspecting $\xi^{-1}(T)$ and $\chi_{\mathbf{Q}}^{-1}(T)$, a clear crossover is found between the high-temperature region ($T > 0.04$), where commensurate AFM fluctuations dominate [maximum of $\chi_{\mathbf{q}}$ at (π, π, π)], to the low-temperature regime ($T < 0.025$) where incommensurate fluctuations at $(\pi, \pi, Q_z < \pi)$ outpace these before approaching the phase transition. At the crossover, ξ^{-1} shows a maximum in Fig. 2, which is, however, not an indication of a decreasing correlation length, but rather reflects the inapplicability of our standard definition of ξ: In the vicinity of the AFM-to-SDW crossover, we have a double-peak structure in $\chi_{\mathbf{q}}$ (not shown) at $Q_z = \pi$ and $Q_z \sim \pi - 0.4$, which altogether appears in the form of a large peak width, i.e., a large ξ^{-1}.

Despite the apparently more complex temperature behavior of ξ and $\chi_{\mathbf{Q}}$, and the onset of an incommensurate order, the critical exponents at low T are not altered at all ($\nu \approx 0.72$, $\gamma \approx 1.42$) with respect to the 3D Heisenberg values. This is ascribed to the persistence of a classical phase transition at $T_N(n = 0.87) \approx 0.012$, which still belongs to the same universality class as the commensurate one. At higher T a linear behavior of the inverse susceptibility (which is characteristic for a mean-field theory for bosonic degrees of freedom) is eventually recovered.

Quantum criticality.—Before turning to our DΓA data at the QCP, let us briefly discuss the analytical results for the nonuniform susceptibility in the random phase approximation (RPA). We start by recalling that the standard HMM approach relies on the expansion [1,5–8]

$$\chi_{\mathbf{Q}+\mathbf{q}}(\omega) = A(\mathbf{q}^2 + \xi^{-2} + i\omega/|\mathbf{q}|^{z-2})^{-1}, \qquad (2)$$

where the first and third term in the denominator are determined by the band dispersion (under the assumption that no Kohn points exist). The T dependence of the correlation length is $\xi^{-1} \propto T^{\nu}$ with $\nu = (d + z - 2)/(2z) = 3/4$ ($d = 3$ and $z = 2$ for a SDW). It originates from the (para)magnon interaction, dominating over the T dependence from the bare susceptibility. Since $d + z > 4$ we are above the upper critical dimension, and quantum criticality can be described by a bosonic mean-field theory.

As shown in the Supplemental Material [54], for the Kohn points on the FS spin fluctuations are, however, enhanced due to their antiparallel Fermi velocities, and their quantum critical behavior changes dramatically. Moreover, as our DΓA calculations below demonstrate, the Kohn quantum critical behavior survives also in the strongly correlated regime. While the (possible) inapplicability of HMM in the presence of Kohn points has been pointed out before [1,8], their implication on the quantum critical behavior in three dimensions and particularly the critical exponents have not been analyzed hitherto.

For the simple cubic lattice, which we consider here for the numerical comparison with the DΓA below, there are

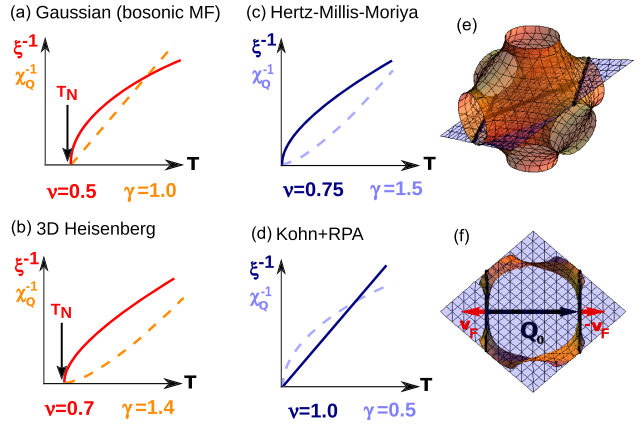

FIG. 3. (a),(b) Magnetic correlation length ξ and magnetic susceptibility $\chi_{\mathbf{Q}}$ vs T comparing the critical exponents ν and γ for a classical finite-temperature phase transition in (a) mean-field theory and (b) for the 3D Heisenberg model. (c),(d) Quantum critical behavior comparing (c) standard HMM theory and (d) our scenario with Kohn line anomaly. (e) Visualization of (one out of four pairs of) Kohn lines in the 3D FS of the simple cubic lattice with nearest-neighbor hopping and the connecting SDW vector $\mathbf{Q}_0$. (f) 2D cut with the Kohn line of (e) and the corresponding (opposite) Fermi velocities.

four pairs of lines of Kohn points $(\pm K_x, \mp K_x - \pi, -Q_z/2)$ and $(\pi \pm K_x, \mp K_x, Q_z/2)$, which are connected by the ground-state spin density wave vectors $\mathbf{Q}_0 = (\pi, \pi, Q_z)$ (and symmetrically equivalent wave vectors) and have opposite Fermi velocity; see Figs. 3(e) and 3(f). The leading contributions in the momentum and T dependence of $\chi_{\mathbf{q}}^{-1}$ are nontrivial already in RPA. They stem from the vicinity of the lines' end points $(0, \pi, \pm Q_z/2)$ and $(\pi, 0, \pm Q_z/2)$, yielding (see Supplemental Material [54])

$$\chi_{\mathbf{Q}_T+\mathbf{q}} \simeq [(\chi_{\mathbf{Q}_0}^{-1})_{T=0} + AT^{1/2} + BT^{-3/2}q_z^2]^{-1}. \quad (3)$$

Here, $\mathbf{Q}_T = \mathbf{Q}_0 + (0, 0, \delta Q_z)$, with $\delta Q_z = -2CT$ describing a shift of the wave vector with the temperature and A, B, C are positive factors, containing weak, $\ln\ln(1/T)$, corrections. The susceptibility Eq. (3) is in stark contrast to the standard expansion Eq. (2). It is strongly anisotropic in momentum and strongly T dependent due to nonanalytic momentum and temperature dependences of the bare susceptibility in the presence of Kohn anomalies. For $q_z = 0$ we obtain the critical exponent $\gamma = 1/2$ for the susceptibility, whereas the critical exponent for ξ (defined in the direction of the z axis) is $\nu = 1$. These exponents are strikingly different from those of HMM theory, $\nu = 3/4$, $\gamma = 2\nu = 3/2$. Even their relative magnitude is reversed; see Figs. 3(c) and 3(d).

A corresponding, radical modification of the critical properties at the QCP (at $n_c = 0.805$) is found also numerically in DΓA, see Fig. 2 (3rd column). Here, the critical exponents change to $\nu = 0.9$ (± 0.1) and $\gamma = 0.6$ (± 0.1) (with an additional error of the same magnitude stemming from the selection of the proper T range, see Fig. 2; a detailed error analysis can be found in the Supplemental Material [54], Sec. II). These exponents are in stark contrast to any standard expectation such as the 3D Heisenberg results or HMM theory, but agree with our RPA exponents. Even when considering the significant error bars, it is safe to say that only the Kohn-anomaly scenario is consistent with our DΓA results as these irrevocably show a roughly linear behavior of $\xi^{-1}(T)$ in the whole low- and intermediate T regime above the QCP (i.e., $\nu \approx 1$) and, even more clear cut, a *strong violation* of the scaling relation $\gamma = 2\nu$ [60], implying a highly nontrivial anomalous dimension η.

Slightly overdoping the system (4th column of Fig. 2, $n = 0.79$) yields a Fermi liquid with a finite $\chi_{\mathbf{Q}}$ for $T \to 0$. In the quantum critical regime (i.e., excluding the low-temperature points which lie outside the quantum critical region) we find similar exponents as at optimal doping ($\nu \approx 1.0$, $\gamma \approx 0.9$; the determination of the accurate value of the critical exponent γ is more difficult because of the restricted temperature range).

No univocal prediction can be made instead for the dynamical exponent z: The frequency dependence of $\chi_{\mathbf{q}}(\omega)$ in the presence of Kohn anomalies has a rather complicated form [23,62], not characterized by a single exponent. The same effect is also responsible for a non-Fermi-liquid power law in the 2D self-energy [23].

Having whole lines of Kohn points and, hence, the above critical exponents is evidently specific to the 3D dispersion with nearest neighbor hopping. Consistent with the results of previous studies [20], however, we demonstrate in Sec. I D of the Supplemental Material [54] that the critical exponents are $\nu = \gamma = 1$ for the more general situations of a FS with isolated Kohn points having opposite masses in two directions. This again violates the HMM prediction. Please note that these values of the exponents in three dimensions coincide (up to logarithmic corrections) [63] with those expected for Kohn points in two dimensions [22].

In general, the momentum dependence of vertex corrections beyond RPA and the self-energy corrections should not be too strong, and the quasiparticle damping should be sufficiently small at $T \to 0$ to preserve the above-mentioned values of the critical exponents in the interacting model. Under these assumptions, we expect the observed behavior to be universal, with several new "universality classes" depending on whether there are lines of Kohn points with divergent or nondivergent mass, or isolated Kohn points with opposite masses (see Supplemental Material [54]).

The final outcome of our calculations, i.e., unusual values of ν, γ and of their mutual relation, which are in a different universality class than HMM theory, can be understood thus as the consequence of two competing physical processes at work: On the one hand, as $T_N \to 0$ at the QCP, the temporal fluctuations increase the effective dimension of the system above the three geometrical ones. This pushes it above the upper critical dimension and renders non-Gaussian fluctuations irrelevant as in HMM. On the other hand, the effect of

Kohn anomalies, yielding a nonanalytic momentum and temperature dependence of the susceptibility, are no longer smeared out by finite T and become relevant.

Conclusions.—We have studied the magnetic QCP in the doped 3D Hubbard model. We find that, even above the upper critical dimension, quantum criticality is not of the standard Hertz-Millis-Moriya type. Even in the presence of strong correlations critical properties are driven by Fermi-surface features: the presence of Kohn points leads to unexpected critical exponents, the breakdown of the scaling relations and not univocal definitions of the dynamical exponent z. The implications of our results go well beyond the specific system considered and also hold for other dispersion relations, showing how strongly the QCP physics can be driven by peculiar features of the FS. In this perspective, the cases where controversial interpretations of experiments in the proximity of QCPs arise might need to be reconsidered.

We thank G. Rohringer, A. Eberlein, W. Metzner, and S. Paschen for insightful discussions. We acknowledge support from the Austrian Science Fund (FWF) through the Doctoral School "Building Solids for Function" (T. S., FWF Project No. W1243), the Project No. I-610 (T. S., A. T.), and Project No. I 1395-N26 as part of the DFG research unit FOR 1346 (K. H.), as well as from the European Research Council under the European Union's Seventh Framework Program (FP/2007-2013)/ERC Grant Agreement No. 306447 (K. H.). The work of A. K. is performed within the theme "Electron" 01201463326 of FASO, Russian Federation and Russian Foundation for Basic Research Grant No. 17-02-00942. Calculations were performed on the Vienna Scientific Cluster (VSC); we thank J. Zabloudil and M. Stöhr for the great support.

[1] H. v. Löhneysen, A. Rosch, M. Vojta, and P. Wölfle, Rev. Mod. Phys. **79**, 1015 (2007).
[2] S. Sachdev, *Quantum Phase Transitions* (Cambridge University Press, Cambridge, England, 1999).
[3] A. Kopp and S. Chakravarty, Nat. Phys. **1**, 53 (2005).
[4] S. Sachdev and B. Keimer, Phys. Today **64**, No. 2, 29 (2011).
[5] T. Moriya and A. Kawabata, J. Phys. Soc. Jpn. **34**, 639 (1973); **35**, 669 (1973); T. Moriya, *Spin Fluctuations in Itinerant Magnetism* (Springer-Verlag, Berlin, Heidelberg, 1985).
[6] I. E. Dzyaloshinskii and P. S. Kondratenko, Sov. Phys. JETP **43**, 1036 (1976).
[7] J. A. Hertz, Phys. Rev. B **14**, 1165 (1976).
[8] A. J. Millis, Phys. Rev. B **48**, 7183 (1993).
[9] R. Jaramillo, Y. Feng, J. Wang, and T. F. Rosenbaumc, Proc. Natl. Acad. Sci. U.S.A. **107**, 13631 (2010).
[10] R. Jaramillo, Y. Feng, J. C. Lang, Z. Islam, G. Srajer, H. M. Ronnow, P. B. Littlewood, and T. F. Rosenbaum, Phys. Rev. B **77**, 184418 (2008).
[11] A. Yeh, Yeong-Ah Soh, J. Brooke, G. Aeppli, T. F. Rosenbaum, and S. M. Hayden, Nature (London) **419**, 459 (2002); M. Lee, A. Husmann, T. F. Rosenbaum, and G. Aeppli, Phys. Rev. Lett. **92**, 187201 (2004).
[12] D. A. Sokolov, M. C. Aronson, L. Wu, Y. Zhu, C. Nelson, J. F. Mansfield, K. Sun, R. Erwin, J. W. Lynn, M. Lumsden, and S. E. Nagler, Phys. Rev. B **90**, 035139 (2014).
[13] A. Schröder, G. Aeppli, R. Coldea, M. Adams, O. Stockert, H. v. Löhneysen, E. Bucher, R. Ramazashvili, and P. Coleman, Nature (London) **407**, 351 (2000).
[14] J. Custers, P. Gegenwart, H. Wilhelm, K. Neumaier, Y. Tokiwa, O. Trovarelli, C. Geibel, F. Steglich, C. P'epin, and P. Coleman, Nature (London) **424**, 524 (2003).
[15] S. Paschen, T. Lühmann, S. Wirth, P. Gegenwart, O. Trovarelli, C. Geibel, F. Steglich, P. Coleman, and Q. Si, Nature (London) **432**, 881 (2004).
[16] Q. Si, S. Rabello, K. Ingersent, and J. Lleweilun Smith, Nature (London) **413**, 804 (2001).
[17] P. Coleman and A. J. Schofield, Nature (London) **433**, 226 (2005).
[18] W. Kohn, Phys. Rev. Lett. **2**, 393 (1959).
[19] L. M. Roth, H. J. Zeiger, and T. A. Kaplan, Phys. Rev. **149**, 519 (1966).
[20] T. M. Rice, Phys. Rev. B **2**, 3619 (1970).
[21] F. Stern, Phys. Rev. Lett. **18**, 546 (1967).
[22] T. Holder and W. Metzner, Phys. Rev. B **85**, 165130 (2012).
[23] T. Holder and W. Metzner, Phys. Rev. B **90**, 161106 (2014).
[24] S. Blundell, *Magnetism in Condensed Matter*, Oxford Master Series in Condensed Matter Physics (Oxford University Press, New York, 2012).
[25] A. Toschi, A. A. Katanin, and K. Held, Phys. Rev. B **75**, 045118 (2007); K. Held, A. A. Katanin, and A. Toschi, Prog. Theor. Phys. Suppl. **176**, 117 (2008).
[26] A. A. Katanin, A. Toschi, and K. Held, Phys. Rev. B **80**, 075104 (2009).
[27] A. Toschi, G. Rohringer, A. A. Katanin, and K. Held, Ann. Phys. (Berlin) **523**, 698 (2011); A. Galler, P. Thunström, P. Gunacker, J. M. Tomczak, and K. Held, Phys. Rev. B **95**, 115107 (2017).
[28] G. Rohringer, Ph.D. thesis, TU Wien (2014).
[29] K. Held, *Dynamical Vertex Approximation*, edited by E. Pavarini, E. Koch, D. Vollhardt, and A. Lichtenstein, Autumn School on Correlated Electrons. DMFT at 25: Infinite Dimensions, Vol. 4 (Forschungszentrum Jülich, 2014), arXiv:1411.5191.
[30] H. Kusunose, J. Phys. Soc. Jpn. **79**, 094707 (2010).
[31] A. N. Rubtsov, M. I. Katsnelson, and A. I. Lichtenstein, Phys. Rev. B **77**, 033101 (2008); H. Hafermann, G. Li, A. N. Rubtsov, M. I. Katsnelson, A. I. Lichtenstein, and H. Monien, Phys. Rev. Lett. **102**, 206401 (2009).
[32] C. Slezak, M. Jarrell, Th. Maier, and J. Deisz, J. Phys. Condens. Matter **21**, 435604 (2009).
[33] A. N. Rubtsov, M. Katsnelson, and A. Lichtenstein, Ann. Phys. (Amsterdam) **327**, 1320 (2012).
[34] G. Rohringer, A. Toschi, H. Hafermann, K. Held, V. I. Anisimov, and A. A. Katanin, Phys. Rev. B **88**, 115112 (2013).
[35] C. Taranto, S. Andergassen, J. Bauer, K. Held, A. Katanin, W. Metzner, G. Rohringer, and A. Toschi, Phys. Rev. Lett. **112**, 196402 (2014); N. Wentzell, C. Taranto, A. Katanin,

A. Toschi, and S. Andergassen, Phys. Rev. B **91**, 045120 (2015).
[36] G. Li, Phys. Rev. B **91**, 165134 (2015).
[37] M. Kitatani, N. Tsuji, and H. Aoki, Phys. Rev. B **92**, 085104 (2015).
[38] T. Ayral and O. Parcollet, Phys. Rev. B **92**, 115109 (2015).
[39] T. Ayral and O. Parcollet, Phys. Rev. B **94**, 075159 (2016).
[40] A. Georges, G. Kotliar, W. Krauth, and M. Rozenberg, Rev. Mod. Phys. **68**, 13 (1996).
[41] W. Metzner and D. Vollhardt, Phys. Rev. Lett. **62**, 324 (1989).
[42] G. Rohringer, A. Valli, and A. Toschi, Phys. Rev. B **86**, 125114 (2012).
[43] T. Schäfer, G. Rohringer, O. Gunnarsson, S. Ciuchi, G. Sangiovanni, and A. Toschi, Phys. Rev. Lett. **110**, 246405 (2013).
[44] G. Rohringer, A. Toschi, A. Katanin, and K. Held, Phys. Rev. Lett. **107**, 256402 (2011); T. Schäfer, A. Toschi, and J. M. Tomczak, Phys. Rev. B **91**, 121107(R) (2015).
[45] A. E. Antipov, E. Gull, and S. Kirchner, Phys. Rev. Lett. **112**, 226401 (2014).
[46] D. Hirschmeier, H. Hafermann, E. Gull, A. I. Lichtenstein, and A. E. Antipov, Phys. Rev. B **92**, 144409 (2015).
[47] T. Schäfer, F. Geles, D. Rost, G. Rohringer, E. Arrigoni, K. Held, N. Blümer, M. Aichhorn, and A. Toschi, Phys. Rev. B **91**, 125109 (2015).
[48] J. Hubbard, Proc. R. Soc. Edinburgh, Sect. A **276**, 238 (1963); M. C. Gutzwiller, Phys. Rev. Lett. **10**, 159 (1963); J. Kanamori, Prog. Theor. Phys. **30**, 275 (1963).
[49] A. L. Rakhmanov, A. V. Rozhkov, A. O. Sboychakov, and Franco Nori, Phys. Rev. B **87**, 075128 (2013).
[50] T. Wu, H. Mayaffre, S. Krämer, M. Horvatić, C. Berthier, W. N. Hardy, R. Liang, D. A. Bonn, and M.-H. Julien, Nature (London) **477**, 191 (2011).
[51] J. Zaanen and O. Gunnarsson, Phys. Rev. B **40**, 7391(R) (1989); K. Machida, Physica (Amsterdam) **158C**, 192 (1989); M. Kato, K. Machida, H. Nakanishi, and M. Fujita, J. Phys. Soc. Jpn. **59**, 1047 (1990).
[52] G. Górski and J. Mozia, Physica (Amsterdam) **409B**, 71 (2013); **87B**, 075128 (2013).
[53] G. Rohringer and A. Toschi, Phys. Rev. B **94**, 125144 (2016).
[54] See Supplemental Material at http://link.aps.org/supplemental/10.1103/PhysRevLett.119.046402 for the detailed calculation of the T and momentum dependence of $\chi_{\mathbf{q}}$ in the presence of Kohn anomalies, which includes Refs. [55,56].
[55] K. Levenberg, Q. Appl. Math. **2**, 164 (1944); D. Marquardt, SIAM J. Appl. Math. **11**, 431 (1963).
[56] T. Schäfer, Ph.D. thesis, TU Wien, Vienna, Austria, 2016.
[57] A. Valli, T. Schäfer, P. Thunström, G. Rohringer, S. Andergassen, G. Sangiovanni, K. Held, and A. Toschi, Phys. Rev. B **91**, 115115 (2015).
[58] G. Li, N. Wentzell, P. Pudleiner, P. Thunström, and K. Held, Phys. Rev. B **93**, 165103 (2016).
[59] J. K. Freericks and M. Jarrell, Phys. Rev. Lett. **74**, 186 (1995); A. N. Tahvildar-Zadeh, J. K. Freericks, and M. Jarrell, Phys. Rev. B **55**, 942 (1997).
[60] Significant violations of $\gamma = 2\nu$, but for a 2D system at $T = 0$, have been recently reported by Maier and Strack [61].
[61] S. A. Maier and P. Strack, Phys. Rev. B **93**, 165114 (2016).
[62] B. L. Altshuler, L. B. Ioffe, and A. J. Millis, Phys. Rev. B **52**, 5563 (1995).
[63] Quantitatively, in two dimensions, $\gamma = 1$ with log corrections [22], differently from the 3D unfrustrated result [$\gamma = 0.5$ with much weaker $\ln\ln(1/T)$ corrections]. The associated second-order transition can be more difficult to realize in two dimensions [62].